

1 *Communication*

2 **Electronic Excitations and Radiation Damage in** 3 **Macromolecular Crystallography**

4 José Brandão-Neto ¹ and Leonardo Bernasconi ²

5 ¹ Diamond Light Source, Diamond House, Harwell Oxford, Didcot OX11 0DE, United Kingdom;
6 jose.brandao-neto@diamond.ac.uk

7 ² Scientific Computing Department, STFC Rutherford Appleton Laboratory, Harwell Oxford, Didcot OX11
8 0QX, United Kingdom; leonardo.bernasconi@stfc.ac.uk

9

10 **Abstract:** Macromolecular crystallography at cryogenic temperatures has so far
11 provided the majority of the experimental evidence that underpins the
12 determination of the atomic structures of proteins and other biomolecular
13 assemblies by means of single crystal X-ray diffraction experiments. One of the
14 core limitations of the current methods is that crystal samples degrade as they are
15 subject to X-rays, and two broad groups of effects are observed: global and specific
16 damage. While the currently successful approach is to operate outside the range
17 where global damage is observed, specific damage is not well understood and may
18 lead to poor interpretation of the chemistry and biology of the system under study.
19 In this work, we present a phenomenological model in which specific damage is
20 understood as the result of a single process, the steady excitation of crystal
21 electrons caused by X-ray absorption, which acts as a trigger for the bulk effects
22 that manifest themselves in the form of global damage and obscure the
23 interpretation of chemical information from XFEL and synchrotron structural
24 research.

25 **Keywords:** Macromolecular crystallography, X-ray diffraction, radiation damage,
26 absorption, electronic excitations, quantum chemistry
27

28 **1. Introduction**

29 Radiation damage in X-ray crystallography has been for a long time an active
30 area of research amongst several groups, but a detailed and general understanding
31 of the physical and chemical mechanisms responsible for the appearance of global
32 or specific damage at a microscopic level is still largely incomplete, even in the case
33 of experiments carried out at cryogenic temperatures. Global damage is
34 characterized by loss of sample diffraction power, indicating reduced crystalline
35 order. Specific damage on the other hand is a local change in the electron density of
36 the crystal constituents around particular atoms of the crystalline structure. In
37 metallo-proteins at 100 K, for instance, it has been shown to involve the reduction of
38 metal ion centres and the formation of radical species at disulphide bonds in the

39 early stages of the experiment [1-4]. These phenomena are then followed by various
40 chemical changes involving, for instance, the elongation and eventual breaking of
41 disulphide bonds, the decarboxylation of glutamate and aspartate residues and the
42 breaking of covalent bonds between the protein backbone and the metal centres.
43 Gerstel et al. [1] provide an exhaustive methodological discussion concerning
44 different susceptibilities empirically observed for all the different types of specific
45 damage described in the literature, while Borek and collaborators recently provided
46 a promising method to discern temperature-dependent changes from other types of
47 change [5]. On the other hand, combined measurements based on single-crystal
48 X-ray diffraction, small angle scattering and radiolysis experiments have shown
49 that hydrogen gas formed in the sample during irradiation, rather than bond
50 cleavage, is mainly responsible for the loss of high-resolution information [6]. *Dose*
51 and *dose rate* are key parameters of the process. *Dose* is the energy absorbed by the
52 material upon irradiation in gray (1 Gy = 1 J/kg) whereas *dose rate* is the power
53 absorbed by the same mass in grays per second (1 Gy/s = 1 W/kg). It is also
54 important to note that historically it is the X-ray *dose* and not the dose rate that is
55 understood to determine damage at cryotemperatures [7], and that, surprisingly,
56 specific damage is observed also in ultra-short (80 fs) X-ray free-electron laser
57 (XFEL) single crystal diffraction experiments [8], performed at room temperature.

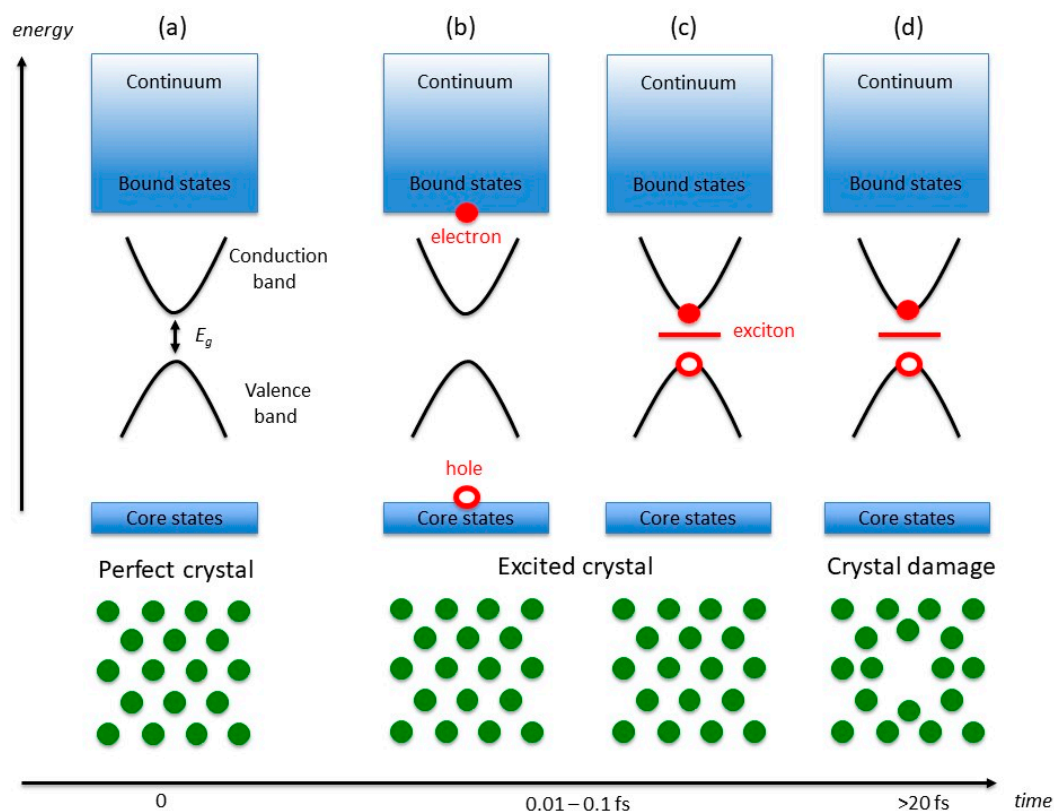
58 Several attempts at rationalizing the radiation-induced structural changes in a
59 crystalline sample have been proposed [e.g. 9-12], typically – but not only - based
60 on purely mechanistic diffusion models, similar to the well-known processes that
61 dominate radiochemistry in solution at room temperature [13]. They are excellent
62 ground work and pragmatically allowed experimenters to steer away from global
63 damage and mapped the bulk of the observable specific damage cases. However,
64 the limitation of the approach is that it cannot explain nor model specific damage,
65 apart from broadly indicating the likely affected parts of a structure. In any case,
66 attempting to perform calculations to understand these effects within a quantum
67 mechanical framework has been impracticable until recently [14].

68 In this work we will outline how specific damage events in crystallographic
69 models can be interpreted in terms of local structural deformations caused by the
70 population and depopulation of virtual and occupied electronic states in the close
71 vicinity of the Fermi energy of the perfect crystal. Previous reports in the literature
72 have addressed and quantified the local changes, but unfortunately, due to the lack
73 of a unifying model, a quantification of this effect has proved to be very subjective
74 and system dependent (although procedures for radiation damage corrections have
75 been refined empirically to a point where a systematic and automated assessment is
76 possible [1, 5, 15]). It is our view that single crystal macromolecular crystallography
77 oscillation datasets are unsuitable for assessing the structural changes caused by
78 specific damage, since they rely on information obtained too long (seconds) after
79 the initial interaction of the X-ray beam with the sample. For long measurement
80 times, the branching of damage events depends both on (1) the type of protein and
81 (2) the actual conditions of the particular samples for each experiment. As we will
82 indicate, over short time-scales (1-10 fs) from the beginning of the experiment, the

83 electronic phenomena mentioned above determine a redistribution of the valence
84 electron density and the appearance of quantum-mechanical forces on the atoms,
85 which, subsequently ($> 10\text{-}20$ fs), drive the evolution of the atomic arrangement and
86 determine the appearance of structural defects and a deviation of the crystal
87 structure from its equilibrium configuration. The model that we propose is based
88 on the wealth of evidence available in the literature [1, 7, 9, 15-20] complemented by
89 our recent study of X-ray radiation damage in *n*-eicosane crystals with
90 quantum-mechanical calculations [14], in which we have demonstrated that the
91 appearance of structural defects following X-ray irradiation is a consequence of (1)
92 the promotion of electrons to low-lying virtual states, (2) the Coulomb interaction of
93 these excited electrons with localized holes at energies comparable to the Fermi
94 energy (excitonic effects), and (3) the structural rearrangement caused by the
95 quantum-mechanical forces induced by the appearance of localized excitonic states.
96 We have also shown that photoemission events do not necessarily lead to structural
97 rearrangement, at least over time-scales of 10-20 fs. The main implication of these
98 findings is that specific radiation damage in simple macromolecules, like
99 *n*-eicosane, occurs at energy scales corresponding to electronic excitations between
100 states very close to the Fermi energy (ca. 0.1-10 eV in semiconducting and insulating
101 crystals) and typical of UV and optical transitions, rather than of photoemission
102 phenomena and core-hole excitations ($10^3\text{-}10^4$ eV). In our model, the electronic and
103 structural changes caused by the interaction of X-rays with a macromolecular
104 crystal structure are therefore akin to typical non-thermal melting phenomena in
105 semiconductors and insulators [21 and Refs. 1-9 therein]. In this communication, we
106 describe a phenomenological model of how different classes of specific damage
107 induced by X-rays can be rationalized in terms of the basic assumptions of this
108 model, and how the appearance of specific damage features in X-ray measurements
109 and sample degradation relate to the timescales of the electronic and nuclear
110 processes described above.

111 2. A Model of Radiation-Induced Structural Changes

112 The central assumption of our model is that radiation damage in
113 macromolecular crystals is related to the generation of bound excitonic states in the
114 forbidden gap region of the perfect crystal. The mechanism leading to the formation
115 of these bound electron-hole pairs is however different from the standard
116 generation of excitons in optical spectroscopy [22], which involves electronic
117 transitions between frontier orbitals (or valence and conduction states) of energies
118 comparable to the band gap of the material (ca. 0.1-10 eV). In typical X-ray
119 experiments, the crystal ground-state electrons (Figure 1 (a)) interact with photons
120 of energies of the order of 10^4 eV, which can either lead to photoemission or to the
121 population of (semi-)bound high-energy conduction states (X-ray absorption), with
122 the simultaneous generation of core holes (Figure 1 (b)).



123

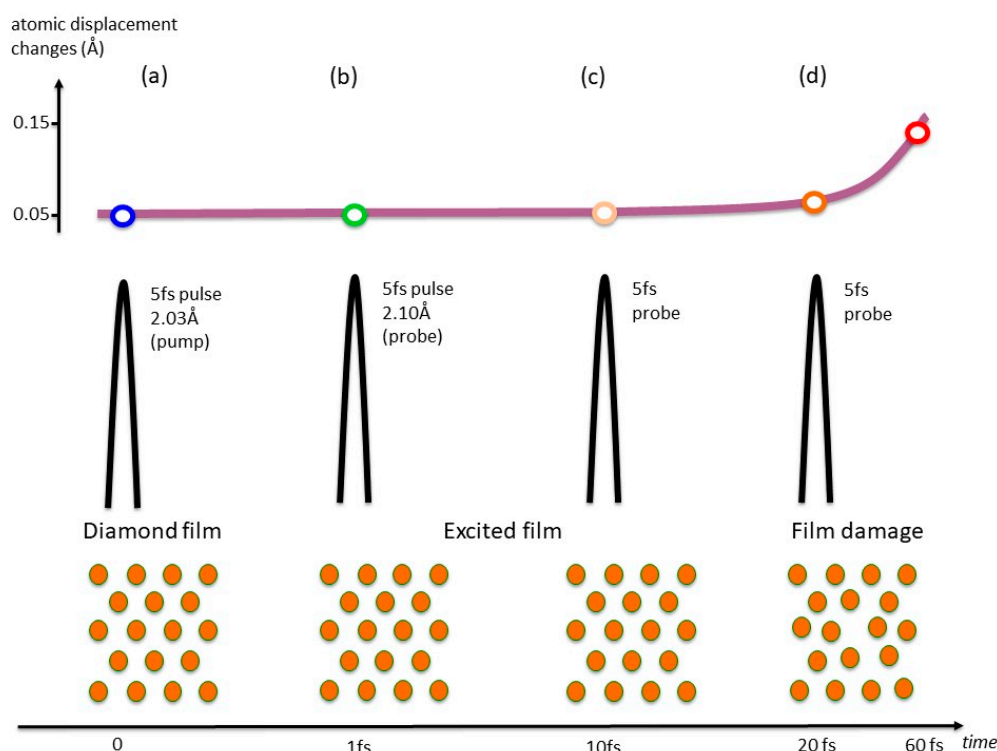
124 **Figure 1.** Electronic energy diagram (top) and atomic position schematic (bottom). The scheme
 125 describes how changes in both the crystal electronic states and atomic positions evolve as X-rays
 126 traverse an insulating crystal. Of particular relevance is the band gap E_g (0.1-10 eV) between the most
 127 energetic electron at the top of the valence band and the energy of a virtual state at the bottom of the
 128 conduction band. Initially (a) all atoms lie in a periodic structure and the electrons populate core and
 129 valence states, up to the Fermi energy. As some X-ray photons are absorbed, electrons are excited
 130 from core states to bound virtual states (b), and counterpart holes are created in the core states. The
 131 excited electrons and holes can form bound excitons (c). If the lifetime of the exciton pair is
 132 sufficiently long (10-100 fs or more), the atomic structure relaxes to screen the exciton (d), which,
 133 macroscopically, determines global changes in the crystalline structure and loss of diffracted
 134 intensity.

135 In typical macromolecular crystallography experiments, which use
 136 (monochromatic) beams of around 13 keV in energy, X-ray absorption accounts for
 137 a total beam loss of ca. 2% for 100 μm thick metal-free crystals, and generates
 138 photoelectrons with kinetic energies comparable to the X-ray photons. The
 139 photoelectrons undergo a fast series of inelastic scattering events that progressively
 140 reduce their energy [23]. These events can be interpreted as a series of transitions
 141 between electronic levels of progressively lower energy, and it can be estimated to
 142 occur within 0.01-0.1 fs in typical experimental conditions [14]. Simultaneously, the
 143 energy of the core hole increases, owing to the many-body electronic screening. For
 144 our purposes, we will assume that the screening is sufficient to create a quasi-hole
 145 in the vicinity of the Fermi energy, which can then form a Coulombically bound
 146 pair with the excited electron and give rise to excitonic intra-gap states (Figure 1
 147 (c)). In consequence to the localised nature of the exciton, strong electron-phonon
 148 interactions couple the nuclear lattice dynamics with the electron-hole pair. The

149 relaxation of the lattice, and the consequent formation of a localised defect in the
150 crystal (Figure 1 (d)), are therefore a consequence of the exciton screening by the
151 crystal phonons and they are promoted by the long lifetimes of excitonic states.

152 This model is consistent with the results of reference [14], in which hybrid
153 time-dependent density-functional theory (TD-DFT) calculations were used to
154 study the time evolution of the crystal structure of *n*-eicosane (C₂₀H₄₂) after X-ray
155 irradiation. An important conclusion of this work is that the presence of a localised
156 electron-hole bound pair is the essential factor driving the structural distortion of
157 the crystal lattice. In the case of a photoexcitation process, in which only the
158 (quasi-)hole is present in the system after irradiation, no formation of localised
159 structural defects was observed in excited-state *ab initio* molecular dynamics
160 (AIMD) simulations (cf. Figure 6 in Ref. [14]). In turn, the resulting change in the
161 crystal symmetry affects the response of the sample to incoming radiation, which
162 can determine changes in measured X-ray structure factors, as well as in a different
163 response of the sample to polarised radiation impinging on different crystal planes
164 during X-ray experiments.

165 One of the defining features of this model is the clear time-scale separation for
166 electronic and nuclear dynamics phenomena. Whereas the charge rearrangement
167 leading to the formation of the exciton pair occurs virtually instantaneously
168 following X-ray absorption (0.01-01 fs) the nuclear relaxation is a relatively slow
169 phenomenon, which, depending on the stiffness of the macromolecular structure,
170 typically cannot occur before at least ca. 10 fs. In the case of *n*-eicosane simulations,
171 the vibrational dynamics of the lattice and the clear nucleation of a defect were
172 observed within ca. 3 ps. As we will indicate below, the presence of two well
173 defined time-scales and physical phenomena leads to the appearance of different
174 forms of radiation damage.



175

176 **Figure 2.** Diagrams with atomic positions and pump-probe pulse structure alongside a graph with
 177 the evolution of the atomic displacement changes measured in a diamond film as the pulses
 178 X-rays traverse the film. Inoue and colleagues [24] determined to what extent a diamond film withstands
 179 X-ray radiation before global atomic position changes result in loss of diffracted signal at room
 180 temperature. Initially there is a periodic lattice, and atomic displacement changes are constant (a). As
 181 X-rays traverse the sample, the atomic positions remain virtually unchanged until ca. 20 ps, when the
 182 nuclei start to move to screen the exciton (electron-phonon interaction). In consequence to the
 183 nuclear rearrangement, non-thermal melting and loss of diffraction intensity are observed.

184 The existence of two well separated time regimes in X-ray induced lattice
 185 changes has been demonstrated in an elegant experiment by Inoue and
 186 collaborators [24], in which an XFEL pump-probe arrangement was used to
 187 examine the dependence of the damage in a diamond film target as a function of
 188 time at room temperature as illustrated in Figure 2. The pump and probe diffraction
 189 intensities were found to be almost constant for at least 20 fs, after which a decrease
 190 in the probed intensity was detected. This indicates that sub-10 fs XFEL pulses can
 191 effectively be used to explore the regime in which only the electronic relaxation
 192 (which, in our model, corresponds to the exciton formation) has occurred. The
 193 results presented in Ref. [14] indicate how these electronic phenomena can be
 194 interpreted, and how they subsequently lead to defect formation, crystal symmetry
 195 reduction and, potentially, changes in the chemical composition of the system (e.g.
 196 bond breaking/formation, evolution of H₂, etc.) [1, 6-8, 15-20].

197 This model can be used to interpret specific radiation damage effects in a
 198 variety of systems. For instance, macromolecular crystals with *metal centres* are the
 199 systems most notoriously affected by X-ray induced damage, and, long before the
 200 appearance of third generation X-ray sources, they have demanded careful

201 consideration for the interpretation of crystallographic models, typically requiring
202 complementary spectroscopic investigations to obtain a satisfactory description of
203 the local metal-centre environment. A widely studied example of this class,
204 investigated by crystallography at cryotemperatures, is the ferryl heme group in
205 peroxidases [4, 18].

206 For moderate to high X-ray doses, a reduction of electron density is observed in
207 the vicinity of the Fe centre during the early stages of a measurement, which
208 essentially results in the "disappearance" of the Fe atoms from the diffraction maps
209 and/or in a change of their oxidation state. Despite all single crystal samples
210 yielding oscillation diffraction datasets with very good quality statistics (ca. 1.6 Å
211 resolution), only at low total dose (20 kGy) the electron density in the vicinity of the
212 Fe centres did not show a reduction compared to crystallographic models, and a
213 multiple-crystal data collection strategy was required [18]. According to our model,
214 the key process induced by the absorption of X-ray photons during irradiation is
215 the excitation of one or more electrons from core and/or valence states of Fe to the
216 conduction band of the crystal, which, in the vicinity of the Fe centre, is likely to
217 possess a predominant heme π^* character. The electron density initially localised on
218 the metal centre is therefore displaced, through a charge-transfer process, to a state
219 delocalised (by conjugation) over the whole heme group. Effectively, this results in
220 the disappearance of electron density at the Fe position, which is then diluted over a
221 much larger volume. This is the factor responsible for the density changes observed
222 for Fe atoms. The formation of a long-lived exciton pair is, in this case, unlikely,
223 since the excited electron lacks localised character. The atomic structure is therefore
224 likely to largely maintain its initial unperturbed configuration (apart from minor
225 variations in bond orders), consistent with the experimental findings. A detailed
226 quantum-mechanical description of this excitation process will be presented
227 elsewhere. In the case of proteins containing *disulphide bonds*, X-ray irradiation can
228 induce S-S bond lengthening or cleavage (along with the formation of radical
229 species) [2]. Early local *ab initio* calculations showed that the bond elongation
230 presents a value consistent with a single electron trapped in the bond, which has
231 been verified more recently in a thorough multi-technique effort using X-ray
232 crystallography, EPR and optical spectroscopy [3]. In our model, these findings can
233 be interpreted in terms of the promotion of one electron from the S-S bond (or from
234 S core states) to the local conduction band, which has σ^* (antibonding) character.
235 This causes a decrease of the bond order, which leads to bond lengthening and,
236 potentially, cleavage. Similarly, the observed rapid decline of electron density in
237 covalent Hg-S bonds [16] can also be interpreted as a consequence of the σ^*
238 (antibonding) character of the excited state resulting in a Hg-S bond lengthening of
239 ca. 7 Å, in conjunction with the mismatch between the original Hg bond
240 environment and the limitations of the atomic distance models used to constrain the
241 structural refinement against the diffraction data.

242 Other cases of X-ray induced radiation damage can similarly be interpreted as a
243 radiation-induced charge-depletion effect in bonding regions of the protein. These
244 include the *decarboxylation of acidic residues* [17]. A thorough assessment of electron
245 density loss in the crystallographic model at carboxyl acidic residue sites was
246 conducted in a variety of local settings within the structure of *Haloarcula marismortui*
247 malate dehydrogenase (HmMD) at 100K. They confirmed that specific damage is
248 most pronounced in acidic side-chains located in the enzymatic active site, followed
249 by acidic residues in the internal cavity formed by the four monomers and those
250 residues involved in crystal contacts. On the other extreme of the scale, HmMD
251 carboxyl bonds mediated by salt bridges are observed to be less sensitive to damage
252 . Similarly, the radiation-induced electron density loss on the -OH group of *tyrosine*
253 residues [20] and the cleavage of methylthio groups in *methionine* can be interpreted
254 as a direct consequence of the electron density rearrangement following excitation
255 to predominately anti-bonding conduction states, which cannot be interpreted by the
256 *a priori* crystallographic models used during the refinement.

257

258 3. Conclusions

259 We have described a new model of X-ray induced damage in macromolecular
260 crystals. Our model is based on experimental work concerning various forms of
261 specific radiation damage and on recent quantum-mechanical calculations on
262 macromolecular crystals. The interaction of X-ray radiation with a sample results in
263 the diffraction, inelastic scattering (Compton effect) or absorption of X-ray photons.
264 The X-ray absorption drives either the photoemission of electrons from the sample,
265 or the creation of electron/hole pairs. In the latter case, the electron and the hole can
266 either remain unbound (e.g. if the electron is promoted to a very delocalized state,
267 as in a conjugated heme system) or form bound pairs (excitons), strongly localised
268 in space, which are characterised by long life times (ca. 1-10 ns, [22]) and whose
269 charge distribution perturbs the atomic arrangement. Over short timescales (up to
270 ca. 10-20 fs), the formation of exciton pairs only involves a redistribution of the
271 electron density, while the nuclear positions remain unchanged relative to their
272 unperturbed geometry. In this situation, localised regions of electronic density
273 depletion can appear (as in the case of peroxidases [18]), which cannot be matched
274 by the global crystallographic models used to refine the crystal structure. For longer
275 time scales, electron-phonon interaction and atomic relaxation can induce
276 substantial rearrangements of the crystal structure, potentially leading to chemical
277 changes in the sample, including bond breaking and the formation of new chemical
278 species (such as H₂) within the crystal. These phenomena are responsible for the
279 occurrence of global damage. It is important to remark that the persistence of
280 localised electron-hole pairs over long times is a *dose-rate independent* phenomenon,
281 in which dose accumulation correlates to the actual atomic displacements within
282 the crystal lattice. Excitons can also act as energy carriers within the
283 macromolecular crystal (e.g. inducing the formation of mobile polaron-like states

284 [25]), and they can be responsible for the energy redistribution in the lattice.
285 Potentially, these approaches can also be extended to the study of the dependence
286 of damage on the wavelength of the applied X-ray radiation, to address longer
287 wavelength regimes which improve the anomalous diffraction signal from weakly
288 diffracting samples [12], or to address the other extreme, short wavelengths for
289 reduced global damage [19]. Computational work on an improved analog system
290 (crystalline sodium acetate tri-hydrate) is currently in progress, which extends the
291 simple alkane model of Ref. [14] to include carboxylic groups and water molecules,
292 providing a better approximation to proteins in the crystal state. Although the
293 model present here is largely qualitative, the theoretical and computational tools
294 developed in recent years to address the structural and dynamic properties of
295 excited states of extended systems [25-27] are paving the way for the development
296 of a general quantitative quantum-mechanical model of radiation damage in X-ray
297 macromolecular crystallography, along the lines indicated in, e.g., Ref. [14], which
298 will provide a robust framework for the interpretation of chemical information
299 from XFEL and synchrotron structural research.
300

301 References

- 302 1. Gerstel, M.; Deane, CM; Garman E.F. Identifying and quantifying radiation damage at the atomic
303 level. *J. Synchrotron Rad.* **2015**, *22*, 201-12.
- 304 2. Weik, M.; Bergès, J.; Raves, M.L.; Gros, P.; McSweeney, S.; Silman, I.; Sussman, J.L.; Houée-Levinh C.;
305 Ravelli, R.B.G. Evidence for the formation of di-sulfide radicals in protein crystals upon X-ray
306 irradiation. *J. Synchrotron Rad.* **2002**, *9*, 342-346.
- 307 3. Sutton K.A., Black P.J., Mercer K.R., Garman E.F., Owen R.L., Snell E.H., Bernhard W.A., Insights into
308 the mechanism of X-ray-induced disulfide-bond cleavage in lysozyme crystals based on EPR, optical
309 absorption and X-ray diffraction studies, *Acta Cryst. D* **2013**, 2381-94.
- 310 4. Moody, P.C.E., Raven, E.L., The Nature and Reactivity of Ferryl Heme in Compounds I and II, *Acc.*
311 *Chem. Res.* **2018**, *51* (2), 427-435.
- 312 5. Borek, D.; Bromberg, R.; Hattne, J.; Otwinowski, Z. Real-space analysis of radiation-induced specific
313 changes with independent component analysis. *J. Synchrotron Rad.* **2018**, *25*, 451-467.
- 314 6. Meents, A.; Gutmann, S.; Wagner, A.; Schulze-Briese, C. Origin and temperature dependence of
315 radiation damage in biological samples at cryogenic temperatures. *PNAS* **2010**, *107*, 1094-1099.
- 316 7. Sliz, P., Harrison, S.C., Rosenbaum, G. How does Radiation Damage in Protein Crystals Depend on
317 X-Ray Dose?, *Structure* **2003**, *11*, 13-19.
- 318 8. Nass, K.; Foucar, L.; Barends, T.R.M.; Hartmann, E.; Botha, S.; Shoeman, R.L.; Doak, R.B.; Alonso-Mori,
319 R.; Aquila, A.; Bajt, S.; Barty, A.; Bean, R.; Beyerlein, K.R.; Bublitz, M.; Drachmann, N.; Gregersen, J.;
320 Jönsson, H.O.; Kabsch, W.; Kassemeyer, S.; Koglin, J.E.; Krumrey, M.; Mattle, D.; Messerschmidt, M.;
321 Nissen, P.; Reinhard, L.; Sitsel, O.; Sokaras, D.; Williams, G.J.; Hau-Riege, S.; Timneanu, N.; Caleman,
322 C.; Chapman, H.N.; Boutet, S.; Schlichting, I. Indications of radiation damage in ferredoxin
323 microcrystals using high-intensity X-FEL beams. *J. Synchrotron Rad.* **2015**, *22*, 225-238.
- 324 9. Helliwell, J.R., Protein Crystal Perfection and the Nature of Radiation Damage, *J. Crystal Growth*, **1988**,
325 *90*, 259-272.
- 326 10. Burmeister, W.P. Structural changes in a cryo-cooled protein crystal owing to radiation damage. *Acta*
327 *Cryst. D* **2000**, *56*, 328-341.
- 328 11. Kmetko, J.; Husseini, N.S.; Naidas, M.; Kalinin Y.; Thorne, R.E. Quantifying X-ray radiation damage in
329 protein crystals at cryogenic temperatures. *Acta Cryst.D* **2006**, *62*, 1030-1038.

- 330
331
332
333
334
335
336
337
338
339
340
341
342
343
344
345
346
347
348
349
350
351
352
353
354
355
356
357
358
359
360
361
362
363
364
365
12. Cianci, M., Helliwell, J.R., Suzuki, A. The interdependence of wavelength, redundancy and dose in sulfur SAD experiments, *Acta Cryst. D*, **2008**, *64*, 1196–1209.
 13. Garman, E.F. Radiation damage in macromolecular crystallography: what is it and why should we care?, *Acta Cryst. D* **2010**, *66*, 339–351.
 14. Bernasconi, L.; Brandao-Neto, J. Radiation damage in X-ray crystallography: a quantum-mechanical study of photoinduced defect formation in beeswax-analogue n-eicosane crystals. *Theor. Chem. Acc.* **2016**, *135*, 1-10.
 15. Bury, C. S., McGeehan, J. E., Antson, A. A., Carmichael, I., Gerstel, M., Shevtsov M. B., Garman, E. F. RNA protects a nucleoprotein complex against radiation damage, *Acta Cryst. D* **2016**, *72*, 648-657.
 16. Ramagopal, U.A.; Dauter, Z.; Thirumuruhan, R.; Fedorov, E.; Almo, S.C. Radiation-induced site-specific damage of mercury derivatives: phasing and implications. *Acta Cryst.* **2005**, *D61*, 1289-1298.
 17. Fioravanti, E.; Vellieux, F.M.; Amara, P.; Madern, D.; Weik, M., Specific radiation damage to acidic residues and its relation to their chemical and structural environment. *J Synchrotron Rad.* **2007**, *14*, 84-91.
 18. Gumiero, A.; Metcalfe, C.L.; Pearson, A. R.; Lloyd Raven, E.; Moody P.C.E. Nature of the Ferryl Heme in Compounds I and II*. *J. Biol. Chem.* **2008**, *286*, 1260-1268.
 19. Fourme, R.; Honkimäki, V.; Girard, E.; Medjoubi, K.; Dhaussy, A.-C.; Kahn, R. Reduction of radiation damage and other benefits of short wavelengths for macromolecular crystallography data collection. *J. Appl. Cryst.* **2012**, *45*, 652-661.
 20. Bury, C.S.; Carmichael I.; Garman, E.F. OH cleavage from tyrosine: debunking a myth. *J. Synchrotron Rad.* **2017**, *24*, 7-18.
 21. Medvedev, N.; Li, Z.; Ziaja, B. Thermal and nonthermal melting of silicon under femtosecond x-ray irradiation. *Phys. Rev. B* **2015**, *91*, 054113.
 22. Rashba, E.I.; Sturge M.D. (eds.), *Excitons*, North Holland Publishing Company, Amsterdam, 1982.
 23. Nave, C.; Hill, M.A. Will reduced radiation damage occur, with very small crystals? *J. Synchrotron Rad.* **2005**, *12*, 299-301.
 24. Inoue, I.; Inubushi, Y.; Sato, T.; Tono, K.; Katayama, T.; Kameshima, T.; Ogawa, K.; Togashi, T.; Owada, S.; Amemiya, Y.; Tanaka, T.; Hara, T.; Yabashi M. Observation of femtosecond X-ray interactions with matter using an X-ray–X-ray pump–probe scheme. *PNAS* **2016**, *113*, 1492–1497.
 25. Bernasconi, L. Chaotic Soliton Dynamics in Photoexcited trans-Polyacetylene. *J. Phys. Chem. Lett.* **2015**, *6*, 908-912.
 26. Runge, E.; Gross, E.K.U. Density-Functional Theory for Time-Dependent Systems. *Phys. Rev. Lett.* **1983**, *52*, 997-1000.
 27. Bernasconi, L.; Tomić, S.; Ferrero, M.; Rérat, M.; Orlando, R.; Dovesi, R.; Harrison, N.M. First principles optical response of semiconductors and oxides. *Phys. Rev. B* **2011**, *83*, 195325.